

# Enhancing array stochastic resonance in ensembles of excitable systems

Fabing Duan<sup>1</sup>, François Chapeau-Blondeau<sup>2</sup> and Derek Abbott<sup>3</sup>

<sup>1</sup> Institute of Complexity Science, Qingdao University, Qingdao 266071, People's Republic of China

<sup>2</sup> Laboratoire d'Ingénierie des Systèmes Automatisés (LISA), Université d'Angers, 62 avenue Notre Dame du Lac, F-49000 Angers, France

<sup>3</sup> Centre for Biomedical Engineering (CBME) and School of Electrical and Electronic Engineering, University of Adelaide, Adelaide, SA 5005, Australia  
E-mail: [fabing1974@yahoo.com.cn](mailto:fabing1974@yahoo.com.cn), [chapeau@univ-angers.fr](mailto:chapeau@univ-angers.fr) and [dabbott@eleceng.adelaide.edu.au](mailto:dabbott@eleceng.adelaide.edu.au)

Received 29 May 2009

Accepted 24 July 2009

Published 18 August 2009

Online at [stacks.iop.org/JSTAT/2009/P08017](http://stacks.iop.org/JSTAT/2009/P08017)

[doi:10.1088/1742-5468/2009/08/P08017](https://doi.org/10.1088/1742-5468/2009/08/P08017)

**Abstract.** A summing network of FitzHugh–Nagumo model neurons, immersed in the background of both external noise and internal noise, is studied in the context of array stochastic resonance. An aperiodic Gaussian stimulus, assisted by collective internal array noise, stimulates the summing network for a more efficient response. This form of array stochastic resonance can be characterized by a correlation coefficient for an aperiodic input signal. Moreover, the correlation gain of the ensembles of neuronal models is investigated for finite and infinite array sizes. The nonmonotonic behavior of the correlation gain and the regions of the correlation gain beyond unity, i.e. the two main features of array SR, are demonstrated numerically and theoretically. These results suggest that certain levels of both external noise and internal noise contribute in a beneficial way to the neuronal coding strategy.

**Keywords:** dynamics (experiment), neuronal networks (theory), signal transduction (experiment), network dynamics

---

**Contents**

<b>1. Introduction</b>	<b>2</b>
<b>2. Dynamics of the FitzHugh–Nagumo model and the correlation gain</b>	<b>4</b>
2.1. Dynamics of the FitzHugh–Nagumo model in the absence of noisy input . . .	5
2.2. Noise-induced spikes in the FitzHugh–Nagumo model . . . . .	6
2.3. Correlation gain for the FitzHugh–Nagumo model in the presence of noisy input . . . . .	7
<b>3. Performance of the neuron arrays with infinite size <math>N \rightarrow \infty</math></b>	<b>9</b>
<b>4. Simulation results</b>	<b>11</b>
<b>5. Array SR theory of an ensemble of FHN neuron models</b>	<b>12</b>
<b>6. Conclusions</b>	<b>15</b>
<b>Acknowledgments</b>	<b>15</b>
<b>References</b>	<b>15</b>

---

**1. Introduction**

Random perturbations may have dramatic effects on dynamical systems and lead to the emergence of new dynamical phenomena, e.g. stochastic resonance (SR) [1]–[10]. The conventional definition of the SR concept was initially limited to transmission of a subthreshold periodic input in a single system mediated via an optimal amount of noise [1, 3, 8]. Over time, the notion of SR has been widened to include a number of different mechanisms [8, 12], and SR effects have also been demonstrated in various systems [8]–[14]. The first non-bistable system, i.e. the FitzHugh–Nagumo (FHN) neuronal model, was discussed in the context of SR by Longtin [11]. Following this, aperiodic SR proposed in the FHN model by Collins *et al* [12] stimulated a number of numerical and theoretical physiological investigations [8], [13]–[18]. Often quite a number of neurons have similar properties and respond to the same stimuli [15], the condition of all neurons in the population having the same pattern of input and output connections were considered in the context of SR [15]–[22], [25]–[27]. However, it has been debated whether the functional role of neuronal noise in biological sensory systems is beneficial for neurons with adaptive capabilities [19, 20]. This discussion was positively answered by an SR-type observation within a population of noisy neurons in a summing network of sensory systems [20]–[22]. Stocks *et al* reported that neuronal noise can have a positive beneficial role, regardless of stimulus intensity or the adaptive capabilities of neurons [19, 20]. The appealing notion of suprathreshold SR might be a reasonable strategy for the enhancement of global correlation in a population of sensory neurons [19]–[22], as SR is only invoked by a subthreshold signal [15], [19]–[21]. An interesting practical application of SR to biomedical engineering is also exploited by Collins *et al* [23, 24], which indicates the noise-enhanced effect is more than just a laboratory curiosity.

J. Stat. Mech. (2009) P08017

In real correlation processing systems, a general condition for a summing network is that each element is driven by not only internal noise, but also a common input signal contaminated by external noise. This configuration has been investigated in non-dynamical and dynamical networks, and the role of internal noise is reported for an improved collective property of the summing network [25]–[30]. In particular, a form of array SR was found by Chapeau-Blondeau *et al* [28], and its main feature is the signal-to-noise ratio gain above unity in a regime of internal noise. In other words, the most interesting point of array SR is the positive role of noise assisting the system output to extract more information from the input [27]–[30]. Thus, it is also of interest to explore how the response of a summing network of sensory systems, to an aperiodic signal corrupted by given external noise, could be maximally enhanced by modulating internal noise. In this regard, some positive results are obtained in the signal transduction by parallel arrays of nonlinear neurons with threshold and saturation [27]. In this paper, we focus on the collective dynamics of a summing network of FHN model neurons in the presence of both external noise and internal noise in the context of array SR. Generally, the measures of the signal-to-noise ratio [8, 10] and the residence-time distribution function [31] are adopted to quantify SR effects in the case of nonlinear systems driven by a periodic input. However, an excitable system, i.e. the FHN model we consider in this paper, is stimulated by an aperiodic stimulus, the interspike interval histogram [11] and the correlation coefficient [12, 13, 15, 16, 32] are commonly employed in these conditions in SR studies. In the present paper, we use the correlation coefficient to characterize the information transmission through ensembles of excitable systems. In order to describe the efficiency of signal transmission through a summing network, we introduce a dimensionless measure of correlation gain, which is the ratio of the correlation coefficient at output to the correlation coefficient at input. Here, the correlation coefficient at output describes the similarity between the aperiodic signal and the network output, while the correlation coefficient at input indicates how similar the initial given noisy input of neurons is to the aperiodic input signal. This kind of information measure was also studied in an array of autoregressive models of order one for a periodic signal [36]. We here numerically simulate the collective response of an ensemble of FHN neuron models to a noisy aperiodic stimulus for different network sizes. The rate expression has been developed by Collins *et al* [12] for analyzing the SR-type behavior in a summing network. Based on Kramers' analysis for the escape rate [12] and our previous study of array SR [30], we further derive an array SR theory considering both two factors of the external noise and the internal noise. This array SR theory can describe the nonmonotonic performance of the correlation gain of an ensemble of FHN neuron models, and also demonstrates a correlation gain that exceeds unity. Furthermore, we demonstrate two optional strategies involving an ensemble of neuronal models: (i) for given external noise plus input signal, the internal noise in a summing network is found to enhance information transmission with correlation gain larger than unity. This strategy represents the adaptive ability of a neuronal population via utilizing its own internal noise; (ii) in the second strategy, the internal noise intensity is fixed, while the external noise can be controlled [25, 26]. As the external noise level increases, the correlation gain is also observed exceeding unity and the information transfer can be improved through the summing network. This strategy indicates that there is an optimal noisy environment for a neuronal population immersed in a given level of internal noise; (iii) additionally, the numerical results demonstrate that

a suprathreshold stimulus can exploit the constructive role of internal noise for obtaining increased information from the response of summing networks. This result agrees with the view of neuronal noise having a positive role for information transmission, regardless of stimulus intensity or the adaptive capabilities of neurons [20].

We assemble the FHN neuron models into a parallel array and investigate the collective response of arrays to a noisy stimulus. The configuration considered in this paper could mimic a sensory neuronal array in building a neural representation of an analog stimulus from the environment. This neural representation is closely related to neuronal inherent nonlinearity, action potentials with short-term firing rate offering a support for signal coding, neuronal ability to operate in arrays, the existence of internal noise, etc. We show that the sensing process can be enhanced by the internal noise in a parallel array. At this sensory level, the performance of the neuronal representation is measured by its ability to obtain a high correlation with the analog stimuli of the environment. We also show that at the optimum point of array SR effect, the array is capable of producing a neural representation that restores a stronger correlation with the information stimulus at the input when this correlation is initially degraded by an external input noise. The present results expressed by the correlation gain are novel and not reported in previous studies of excitable systems [11]–[13], [15]–[20]. Although this process we describe in the present paper is at an early stage of the neural information processing chain, we argue that it is an important part of the neuronal information processing at the sensory level.

## 2. Dynamics of the FitzHugh–Nagumo model and the correlation gain

We consider a summing network of identical FHN model neurons given as

$$\begin{aligned}\varepsilon \frac{dv_i}{dt} &= f(v_i) - w_i + A + b + s(t) + \xi(t) + \eta_i(t), \\ \frac{dw_i}{dt} &= v_i - \gamma w_i,\end{aligned}\tag{1}$$

where  $f(v) = v(a-v)(v-1)$ ,  $\gamma, \varepsilon > 0$ ,  $0 < a < 1$  and  $i = 1, 2, \dots, N$ . Here,  $v(t)$  models the membrane potential and  $w(t)$  plays the role of a recovery variable incorporating channel gating dynamics. All neurons are subjected to the same aperiodic Gaussian signal  $s(t)$  plus external noise  $\xi(t)$ , given that real-world external signals are often aperiodic [15]. Here,  $s(t)$  is formed by prefiltering a Gaussian random signal with correlation time  $\tau_s$  and average signal variance  $\sigma_s^2$ , as shown in figure 3(a). The autocorrelation of  $s(t)$  is  $\langle s(t)s(t') \rangle = \sigma_s^2 \exp(-|t - t'|/\tau_s)$ , and the brackets  $\langle \cdot \rangle$  denote an ensemble average. The exact form of  $s(t)$  is unimportant, provided its variations occur on a timescale which is slower than the characteristic time of the FHN system under study [11, 15]. According to the original study of SR in the FHN model, the timescale of input stimulus should be much larger than the timescale of the membrane potential  $v(t)$ , i.e. the timescale of  $\varepsilon$  [11]. In the following numerical simulations,  $s(t)$  can be viewed as a slow stimulus with the correlation time  $\tau_s = 20$  s, in comparison with the timescale parameter of  $\varepsilon = 0.05$  s. Here,  $\xi(t)$  is zero-mean Gaussian white noise with intensity  $2D_\xi$ . At the same time, zero-mean Gaussian white internal noise  $\eta_i(t)$ , together with and independent of  $s(t) + \xi(t)$ , is applied to each element of the summing network of size  $N$ . The  $N$  internal noise terms  $\eta_i(t)$  are mutually independent and have autocorrelation  $\langle \eta_i(t)\eta_i(0) \rangle = 2D_\eta \delta(t)$  with the

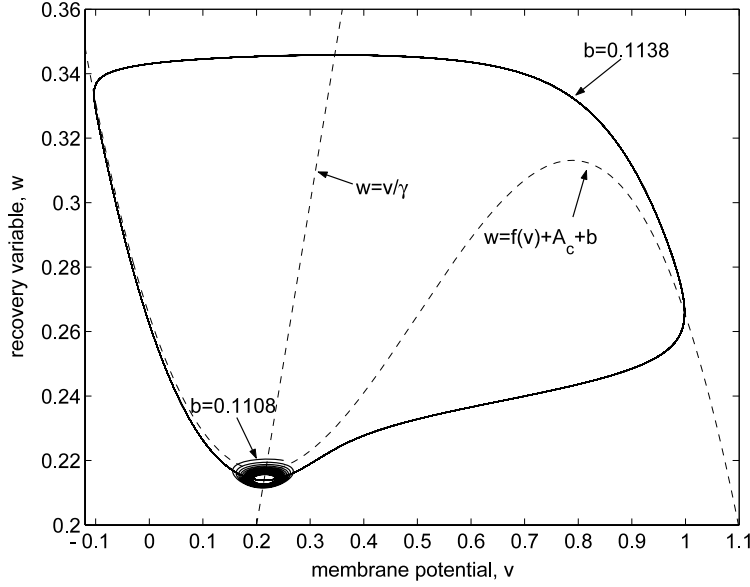


**Figure 1.** The dependence of the trajectories and the appearance of Canard trajectories on the parameter  $b$  in the FHN model in the absence of noise and input signal. The dashed lines are the two nullclines of  $w = f(v) + A_c + b$  and  $w = v/\gamma$ . The trajectories for  $b = 0.1108 < b_{th}$  and  $b = 0.1138 > b_{th}$  are pointed by arrows, respectively.

same noise intensity  $2D_\eta$ . Note that, if a sampling time  $\Delta t$  is adopted, the Gaussian white noise terms  $\xi(t)$  and  $\eta_i(t)$  have a variance of  $\sigma_\xi^2 = 2D_\xi/\Delta t$  and  $\sigma_\eta^2 = 2D_\eta/\Delta t$ , respectively [28, 29].

### 2.1. Dynamics of the FitzHugh–Nagumo model in the absence of noisy input

In the absence of the noise and the input signal, we assume a unique fixed point  $(v^*, w^*)$ , i.e. the real solution of the cubic equation of  $f(v^*) - w^* + A = 0$  and  $w^* = v^*/\gamma$ . The stability of the equilibrium point is determined by the Jacobian matrix

$$J = \begin{pmatrix} f'(v^*)/\varepsilon & -1/\varepsilon \\ 1 & -\gamma \end{pmatrix}. \quad (2)$$

The constant activation signal  $A$  is chosen at the Hopf bifurcation point defined by  $\text{Tr}(J) = 0$  and  $\det(J) > 0$ , which yields  $f'(v^*) = \varepsilon\gamma$  and the fixed point  $(v^* = [(a+1) - (a^2 - a + 1 - 3\varepsilon\gamma)^{1/2}]/3, w^* = v^*/\gamma)$ . Thus, a supercritical Hopf bifurcation point of the activation signal  $A$  is at

$$A_c = [(a^2 - a + 1 - 3\varepsilon\gamma)^{1/2} \times (2\gamma a^2 - 2\gamma a + 2\gamma + 3\varepsilon\gamma^2 - 9) + 9a + 9 + \gamma(-2a^3 + 3a^2 + 3a - 2)]/(27\gamma). \quad (3)$$

Throughout this paper, the value of  $A = A_c$ . However, a spike is only deemed to be transmitted if the oscillations (spikes) grow beyond a given level of  $v_{th}$ , otherwise the transmitted response is taken to be zero [12, 15, 20]. In this paper, the given threshold level  $v_{th} = a$  and firing events only occur when  $b$  is above the threshold  $b_{th}$ . In this

situation, the input signal  $s(t)$  is defined as a suprathreshold signal in the sense that a deterministic threshold crossing occurs [12], i.e.  $b + s(t) \geq b_{\text{th}}$ , otherwise the input signal is subthreshold. In order to estimate the crossing threshold  $b_{\text{th}}$ , the FHN model (1) can be transformed as

$$\varepsilon \frac{dv'}{dt} = f(v') - w' + b', \quad \frac{dw'}{dt} = v' - \gamma w' - (1 - \gamma)a, \quad (4)$$

using the following transformations:

$$v \rightarrow v' + a, \quad w \rightarrow w' + a, \quad b \rightarrow b' - A_c + a. \quad (5)$$

Like the above linear stability analysis of the activation signal  $A_c$ , we determine the minimum of the nullcline occurring at  $v_- = -\sqrt{1 - 4\varepsilon}/(2\sqrt{3})$ , and the threshold voltage  $b'_{\text{th}} = -(5 - 2\varepsilon)\sqrt{1 - 4\varepsilon}/(12\sqrt{3})$ . Throughout this paper, each FHN neuron model of the summing network takes  $a = 0.5$ ,  $\gamma = 1$ ,  $\varepsilon = 0.005$ ,  $A_c = 0.1512$  and the sampling time  $\Delta t = 0.001$  s in simulation tests. Then, the threshold  $b'_{\text{th}} = -0.2377$  and  $b_{\text{th}} = b'_{\text{th}} - A_c + a$  takes as 0.1111.

When the constant activation signal  $A$  is chosen at the Hopf bifurcation point  $A_c = 0.1512$ , a Canard-like behavior of FHN neuron model is crucially dependent on the parameter  $b$  [13, 34]. Two examples of Canard trajectories on the parameter  $b$  in the FHN model are depicted in the phase plane of  $(v, w)$  in figure 1. The dashed lines are the two nullclines of  $w = f(v) + A_c + b$  and  $w = v/\gamma$ . The trajectories for  $b < b_{\text{th}}$  and  $b > b_{\text{th}}$  are indicated by arrows in figure 1, respectively. When the parameter  $b = 0.1108 < b_{\text{th}}$ , a Canard solution of the FHN neuronal model follows a repelling slow manifold for a considerable amount of time [13, 34]. In this case, the membrane potential  $v(t)$  is below the assumed threshold  $v_{\text{th}} = 0.5$ . As  $b = 0.1138 > b_{\text{th}}$ , a large excursion loop is excited, as shown in figure 1, and a spike train comes into being as the membrane potential  $v(t)$  exceeds  $v_{\text{th}} = 0.5$  circularly [13, 34, 35].

## 2.2. Noise-induced spikes in the FitzHugh–Nagumo model

Noise permeates every level of the nervous system and poses a fundamental problem for information processing. In contrast to the linear systems, noise is regarded as a beneficial factor that affects the performance of nonlinear systems. The constructive role of noise in the FHN model has been extensively investigated in the context of stochastic resonance or coherence resonance [8], [10]–[13], [15]–[18], [20, 33]. For a given amount of internal noise  $\eta_i(t)$  only ( $2D_\eta = 10^{-7}$ ,  $D_\xi = 0$  and  $s(t) \equiv 0$ ), a stochastic realization of noise-induced excursions of a single FHN model through the phase plane is shown in figure 2(a) and the corresponding spike train in the membrane potential  $v(t)$  is illustrated in figure 2(b). For comparison, the oscillation of the FHN model without noise is also plotted by solid lines in figure 2. It is seen that, even as  $b = 0.1108 < b_{\text{th}}$  and a deterministic trajectory in the phase plane is below the threshold  $v_{\text{th}} = 0.5$ , the injection of noise  $\eta_i(t)$  helps the membrane potential  $v(t)$  cross the threshold  $v_{\text{th}}$ . Thus, due to noise fluctuation, the corresponding crossing events become possible, which are recoded as a spike train resembling the spontaneous activity of an FHN model [13].

In the presence of both input signal and noise, the occurrence of spikes will be correlated with this input signal. In section 2.3, we will study this correlation between the FHN model response and the noisy input, yielding the resonance-like behavior of the correlation gain versus the noise intensity.

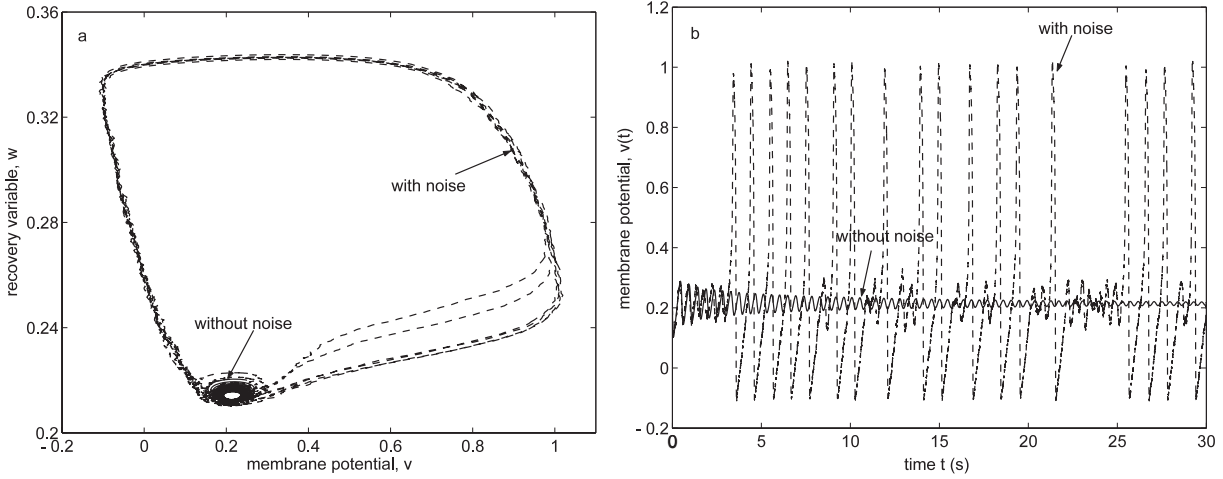


**Figure 2.** (a) Occurrence of spike in a noise-driven FHN model (dashed line) and oscillation of FHN model without noise (solid line) in the phase plane of  $(v, w)$ ; (b) the corresponding time evolution of membrane potential  $v(t)$  to the presence of noise (dashed line) and the absence of noise (solid line). Here, the noise density  $2D_\eta = 10^{-7}$  and  $b = 0.1108$ .

### 2.3. Correlation gain for the FitzHugh–Nagumo model in the presence of noisy input

In the presence of the noisy input signal  $s(t) + \xi(t) + \eta_i(t)$ , each FHN model of (1) presents its response  $v_i(t)$ . These outputs of a summing network of FHN neurons are summed together to yield the network response  $\tilde{r}(t) = \sum_{i=1}^N v_i(t)/N$ . The response  $\tilde{r}(t)$  is filtered by a 10 s unit-area symmetric Hanning window for obtaining the firing rate  $r(t)$  [12, 37], e.g. figures 3(b) and (c).

We characterize the global information transmission through the network by the correlation coefficient of the input  $s(t)$  and the firing rate  $r(t)$  [12, 28]:

$$\rho_{s,r} = \frac{\overline{(s(t) - \overline{s(t)})(r(t) - \overline{r(t)})}}{\sigma_s \left[ \overline{(r(t) - \overline{r(t)})^2} \right]^{1/2}} = \frac{\overline{s(t)r(t)}}{\sigma_s \left[ \overline{(r(t) - \overline{r(t)})^2} \right]^{1/2}}, \quad (6)$$

where the overbar indicates an average value of a random variable over time and the deterministic signal  $s(t)$  is with  $\overline{s(t)} = 0$  [12, 28]. We also consider the correlation coefficient of the net input signal  $s(t)$  and the initial given noisy input  $s(t) + \lambda(t)$  as

$$\rho_{s,s+\lambda} = \frac{\sigma_s}{(\sigma_s^2 + \sigma_\lambda^2)^{1/2}}, \quad (7)$$

where the term  $\lambda(t)$  represents the controllable noise term, for example,  $\lambda(t)$  is  $\xi(t)$  if  $\eta_i(t)$  is fixed, or vice versa. Here, we emphasize that the correlation coefficient  $\rho_{s,s+\eta}$  can be computed by any internal noise  $\eta_i(t)$ , since each initial given noise  $\eta_i(t)$  has the same noise density of  $2D_\eta$ , as discussed in figure 4. Thus, we define the correlation gain  $G$  as

$$G = \frac{\rho_{s,r}}{\rho_{s,s+\lambda}} = \frac{\overline{s(t)r(t)}}{\left[ \overline{(r(t) - \overline{r(t)})^2} \right]^{1/2}} \times \frac{(\sigma_s^2 + \sigma_\lambda^2)^{1/2}}{\sigma_s^2}, \quad (8)$$

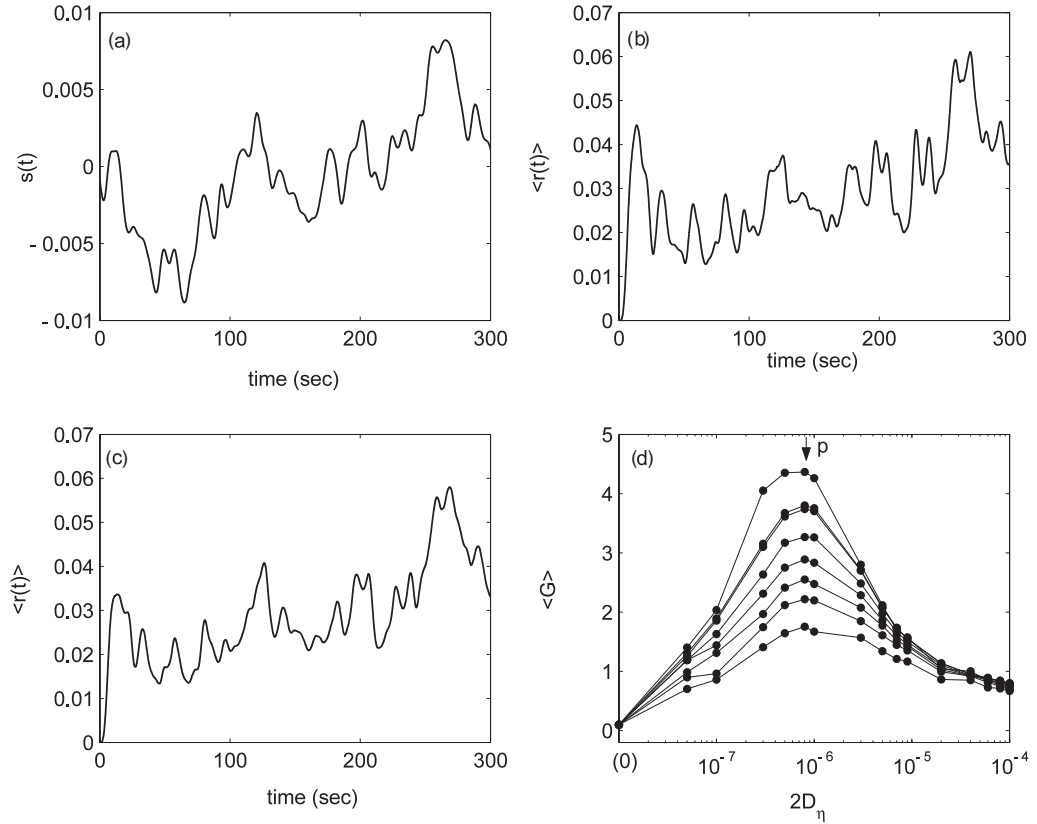


**Figure 3.** (a) An aperiodic Gaussian signal  $s(t)$  formed by prefiltering Gaussian noise with correlation time  $\tau_s = 20$  s. Here, the average signal variance  $\sigma_s^2 = 1.5 \times 10^{-5}$  and total time length 300 s; (b) ensemble-average values of the firing rate  $r(t)$ , at the point  $p$  of (d) (as indicated by the arrow), is obtained by filtering the response  $\tilde{r}(t) = \sum_{i=1}^N v_i(t)/N$  with a 10 s unit-area symmetric Hanning window for the neuron array size  $N = 120$ . Here, the resonance point  $p$  corresponds to the internal noise density  $2D_\eta = 8 \times 10^{-7}$ ; (c) ensemble-average values of the firing rate  $r(t)$  as the neuron array size  $N \rightarrow \infty$  at the point  $p$  indicated in (d). In numerical simulations, we take  $(\sum_{i=1}^K r_i(t) \sum_{j=K+1}^{2K} r_j(t)/K^2)^{1/2}$  as the approximate ensemble-average value of the firing rate  $r(t)$  of the infinite neuron array with size  $N \rightarrow \infty$ . Here, we take  $K = 120$ ; (d) ensemble-average values of the correlation gain  $G = \rho_{s,r}/\rho_{s,s+\xi}$  as a function of the internal noise density  $D_\eta$  for the network with  $N = 1, 2, 3, 5, 10, 60, 120$  and  $\infty$  neurons (from the bottom up). Here, the external noise density  $2D_\xi = 3 \times 10^{-7}$ ,  $A_c = 0.1512$ ,  $b = 0.07$  and the sampling time  $\Delta t = 0.001$  s. The input signal  $s(t)$  is then subthreshold as  $b + s(t) < b_{th} = 0.1111$ . For simplicity, we represent the origin tick  $10^{-8}$  of the logarithmic  $x$  axis as zero, and all curves of the correlation gain  $G$  start at  $D_\eta = 0$  actually. It is shown that the correlation gain  $G \sim 0.098$  at  $D_\eta = 0$ , because a small dose of external noise  $\xi(t)$  is already added ( $2D_\xi = 3 \times 10^{-7}$ ). Each point was averaged by 200 trials in the realization of simulations and the Gaussian white noise is generated with different seeds.



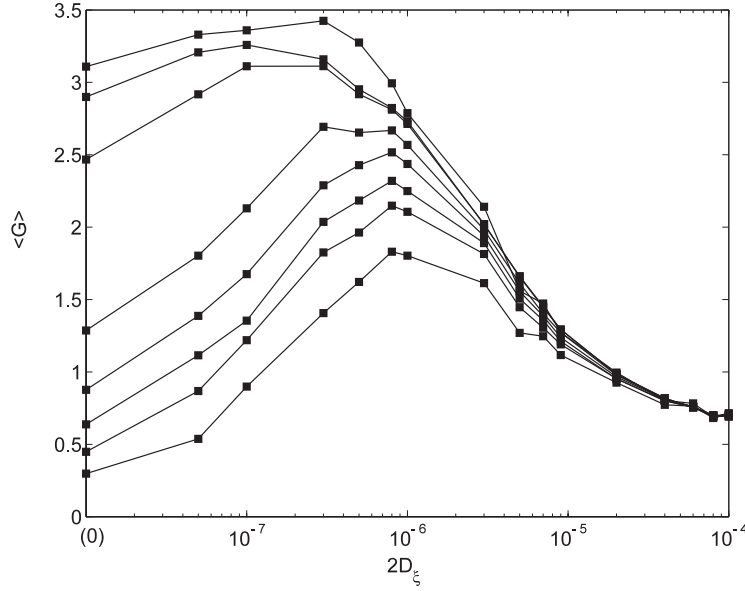


**Figure 4.** Ensemble-average values of the correlation gain  $G = \rho_{s,r}/\rho_{s,s+\eta}$  as a function of the internal noise density  $D_\xi$  for the network with  $N = 1, 2, 3, 5, 10, 60, 120$  and  $\infty$  neurons (from the bottom up). Here, the internal noise density  $2D_\eta = 3 \times 10^{-7}$  is fixed and other parameters are the same as in figure 3. For simplicity, we represent the origin tick  $10^{-8}$  of the logarithmic  $x$  axis as zero, and all curves of the correlation gain  $G$  start at  $D_\xi = 0$  actually.

for evaluating the positive role of internal or external noise in the summing network of FHN model neurons.

### 3. Performance of the neuron arrays with infinite size $N \rightarrow \infty$

Assume the impulse function of filter is  $h(t)$ , each neuron output  $v_i(t)$  is then filtered as its firing rate  $r_i(t) = h(t)v_i(t)$ , and the firing rate of the summing network  $r(t) = \sum_{i=1}^N r_i(t)/N$ . Equation (6) can be further deduced as

$$\begin{aligned}
 \rho_{s,r} &= \frac{\overline{s(t) \sum_{i=1}^N r_i(t)/N}}{\sigma_s \left[ \left( \overline{\sum_{i=1}^N r_i(t)/N} - \overline{\sum_{i=1}^N r_i(t)/N} \right)^2 \right]^{1/2}} \\
 &= \frac{\overline{s(t)r_i(t)}}{\sigma_s \left[ (N\overline{r_i^2(t)} + N(N-1)\overline{r_i(t)r_j(t)})/N^2 - (N\overline{r_i(t)}^2)/N^2 \right]^{1/2}} \\
 &= \frac{\overline{s(t)r_i(t)}}{\sigma_s \left[ \overline{r_i^2(t)} - \overline{r_i(t)}^2 - \overline{r_i(t)r_j(t)}/N + \overline{r_i(t)r_j(t)} \right]^{1/2}}, \tag{9}
 \end{aligned}$$

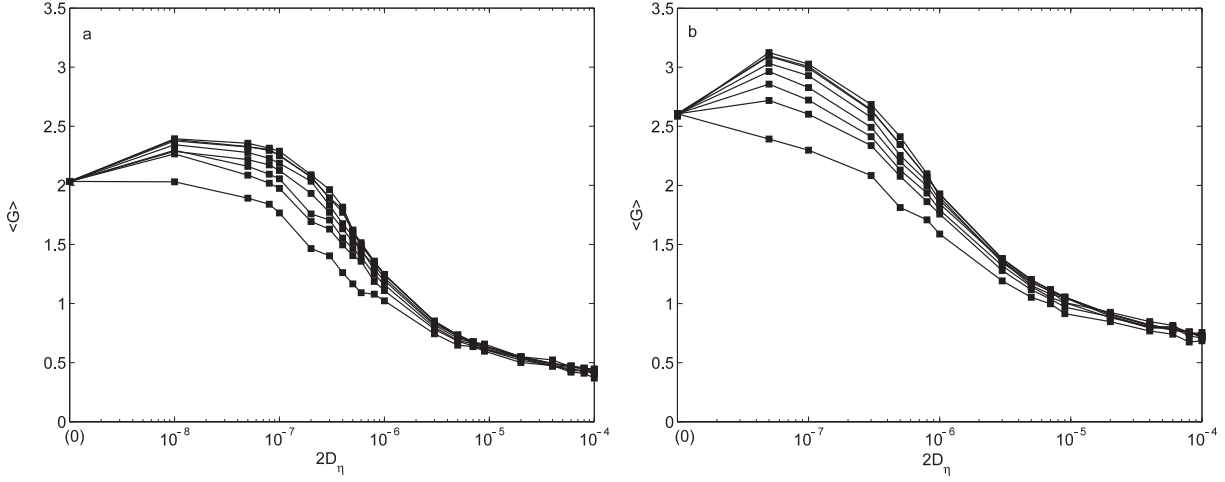


**Figure 5.** Ensemble-average values of the correlation gain  $G = \rho_{s,r}/\rho_{s,s+\xi}$  as a function of the internal noise density  $D_\eta$  for the network with  $N = 1, 2, 3, 5, 10, 60, 120$  and  $\infty$  neurons (from the bottom up) with a given external noise density (a)  $2D_\xi = 10^{-7}$  and (b)  $2D_\xi = 3 \times 10^{-7}$ . Here,  $b = 0.1217$  and  $s(t)$  is a suprathreshold signal as  $b + s(t) > b_{\text{th}} = 0.1111$ . Other parameters are the same as in figure 3. For simplicity, we represent the origin tick  $10^{-9}$  in (a) ( $10^{-8}$  in (b)) of the logarithmic  $x$  axis as zero, and all curves of the correlation gain  $G$  start at  $D_\eta = 0$  actually.

with  $i \neq j$  and  $i, j = 1, 2, \dots, N$ . Thus, for the infinite array size  $N \rightarrow \infty$ , we have the correlation coefficient of the input  $s(t)$  and the firing rate  $r(t)$  as

$$\lim_{N \rightarrow \infty} \rho_{s,r} = \frac{\overline{s(t)r_i(t)}}{\sigma_s \left[ \overline{r_i(t)r_j(t)} \right]^{1/2}}, \quad (10)$$

and the correlation gain  $G$  as

$$\lim_{N \rightarrow \infty} G = \frac{\rho_{s,r}}{\rho_{s,s+\lambda}} = \frac{\overline{s(t)r_i(t)}}{\sigma_s^2} \times \frac{(\sigma_s^2 + \sigma_\lambda^2)^{1/2}}{\left[ \overline{r_i(t)r_j(t)} \right]^{1/2}}. \quad (11)$$

Since the indices  $i$  and  $j$  are different, but arbitrary in (10) and (11), we can adopt two different FHN neuron models, each embedded with independent internal noise  $\eta_i(t)$  ( $\eta_j(t)$ ), to evaluate the correlation coefficient or gain of the ensemble of neuron arrays with size  $N \rightarrow \infty$ , as shown in figures 3–5. This method is tractable and effective in simulation tests and has been testified in evaluating the signal-to-noise ratio gain [29].

Note that the neuronal spikes are depicted and counted when  $v(t)$  crosses the given threshold voltage  $v_{\text{th}} = a$  ( $a > 0$ ), so the network response  $r(t) \geq 0$  after filtering the neuronal spikes by a 10 s unit-area symmetric Hanning window. Furthermore, following the deduction of the infinite array size  $N \rightarrow \infty$ , we can extract  $r(t)$  of an infinite neuronal

array as

$$\begin{aligned}
 \lim_{N \rightarrow \infty} r(t) &= \lim_{N \rightarrow \infty} \sum_{i=1}^N r_i(t)/N \\
 &= \lim_{N \rightarrow \infty} \left[ \frac{\sum_{i=1}^N r_i(t) \sum_{i=1}^N r_i(t)}{N^2} \right]^{1/2} \\
 &= \lim_{N \rightarrow \infty} \left[ \frac{r_i^2(t) + (N-1)r_i(t)r_j(t)}{N} \right]^{1/2} \\
 &= [r_i(t)r_j(t)]^{1/2}, \tag{12}
 \end{aligned}$$

with  $i \neq j$  and  $i, j = 1, 2, \dots, N$ . Therefore, we can also obtain the ensemble-averaged firing rate of an infinite neuronal array by utilizing two arbitrary but different response of neuronal models, e.g. an ensemble-averaged example of firing rate illustrated in figure 3(c). In numerical simulations, we can take  $(\sum_{i=1}^K r_i(t) \sum_{j=K+1}^{2K} r_j(t)/K^2)^{1/2}$  as the approximate ensemble-average value of the firing rate  $r(t)$  for an infinite array with size  $N \rightarrow \infty$ , as shown in figure 3(c).

#### 4. Simulation results

The input signal  $s(t)$ , as shown in figure 3(a), is subthreshold for  $b_{th} = 0.1111$ , since  $b = 0.07$  and  $\sigma_s^2 = 1.5 \times 10^{-5}$ . Note that  $s(t)$  is corrupted by a given external noise  $\xi(t)$  with density  $2D_\xi = 3 \times 10^{-7}$ , yielding the correlation coefficient  $\rho_{s,s+\xi} = 0.2182$ . Figure 3(d) plots the correlation gain  $G = \rho_{s,r}/\rho_{s,s+\xi}$  as a function of internal noise density  $D_\eta$  for different array sizes  $N = 1, 2, 3, 5, 10, 60, 120$  and  $\infty$  (from the bottom up). As the level of internal noise  $\eta_i(t)$  increases from zero, the feature of array SR is obvious, i.e. the bell-type curve of  $G$  versus  $D_\eta$ , as illustrated in figure 3(d). Moreover, the collective property of the internal noise enhances array SR as the neuronal array size  $N$  increases. We emphasize these characteristics: (i) the correlation gain  $G$  is larger than unity in certain regimes of internal noise density of  $D_\eta$ , as shown in figure 3(d). This indicates the neuronal array has an optional route to maximize the global information transmission via array SR; (ii) when the internal noise increases from zero, the correlation gain  $G$  of the summing network with different size  $N$  comes from a same but nonzero value. At the zero value of internal noise density ( $D_\eta = 0$ ), all neurons receive a common noise input  $s(t) + \xi(t)$ , and the collective effect of the summing network is invalid. This property is not limited to the subthreshold input signal  $s(t)$  shown in figure 3(d) and is also observed for the suprathreshold signal  $s(t)$  in figure 5. (iii) When the neuronal array size  $N \rightarrow \infty$ , the firing rate  $r(t)$  is numerically shown in figure 3(c). With the help of internal array noise  $\eta_i(t)$ , the ensemble-average value of the correlation coefficient  $\rho_{s,r}$  can reach as high as 0.9528 and the correlation gain  $G \sim 4.3666$  at the resonant point of  $2D_\eta = 8 \times 10^{-7}$ , as illustrated in figure 3(d).

Figure 3(d) manifests an adaptive strategy for a neuronal population in a given noisy environment, i.e. adjusting the intensity of internal noise  $\eta_i(t)$  to improve the global information transmission. Another important case is when the level of internal noise of a neuronal population is fixed, while the external noise  $\xi(t)$  acts as a controllable variable for

optimizing the global correlation transmission [25, 26], as shown in figure 4. From figure 4, the correlation gain  $G$  also shows the resonance curve as a function of the external noise density  $D_\xi$ . This effect is also enlarged by increasing the size of the summing network  $N$ . But a crucial difference is that each resonance curve starts at different points for different array sizes  $N$ . At the start,  $D_\xi = 0$  and the mutual independent internal noise  $\eta_i(t)$  enhances the collective effect as  $N$  increases; this reduces to the cases considered in [15, 20]. In other words, the spike events, invoked by internal noise  $\eta_i(t)$ , assemble at the output for obtaining more pronounced correlation. As the external noise density  $D_\xi$  increases, the presence of both external and internal noise leads to array SR, as plotted in figure 4.

A criticism of SR was that an adaptive neuron can adjust its threshold for improving information transmission, and this fact leads to the conclusion of SR being redundant in a single neuron. This argument is addressed by the mechanism of suprathreshold SR in [19, 20]. Namely, the internal noise, independent of the threshold setting, is observed to be of benefit for both subthreshold and suprathreshold signals [19, 20]. For the appearance of both external and internal noise considered in this paper, this kind of observation is affirmed again. Figure 5 shows the noise dependence of the global correlation transmission for the suprathreshold stimulus corrupted by the given external noise  $\xi(t)$ . It is interesting to note that the correlation gain  $G$  can also be larger than unity and enhanced by the array size  $N$ . Array SR enables the constructive role of internal noise to manifest for suprathreshold signal, even if the SR effect disappears in a single neuron model ( $N = 1$ ). It is observed in figure 5 that array SR appears as the size of summing network  $N$  increases, and the positive beneficial role neuronal internal noise does play in the neuronal population, regardless of the adaptive capabilities of single neurons [19, 20].

## 5. Array SR theory of an ensemble of FHN neuron models

The theoretical Kramer-type analysis of the ensemble-averaged rate has been developed by Collins *et al* for a single excitable system [12] and a summing network of excitable systems [15]. In the presence of both the external noise and the internal noise, an approximation theory of array SR was proposed in a parallel array of bistable systems [30]. We here, combining the proposed theories of [12, 30], interpret the aforementioned numerical results of array SR in the ensemble of FHN neuron models theoretically. This array SR theory for the ensembles of FHN neuron models can approximately explain the roles of the external noise and the internal noise, and describes the performance of the summing network with different array sizes.

We rewrite (4) taking account of the threshold voltage  $b'_{th}$  and the stimulus  $s(t)$  [12]:

$$\begin{aligned} \varepsilon \frac{dv'_i}{dt} &= -v'_i \left( v'^2_i - \frac{1}{4} \right) - w'_i + b'_{th} - B + s(t) + \xi(t) + \eta_i(t), \\ \frac{dw'_i}{dt} &= v'_i - w'_i, \end{aligned} \tag{13}$$

with parameters  $\varepsilon = 0.005$ ,  $a = 1/2$  and  $\gamma = 1$ . Here,  $B = b_{th} - b$  is a constant parameter which corresponds to the signal-to-threshold distance. Using the Kramers' formula, the

ensemble average of the escape rate of  $r_i(t)$  of a single neuron is derived as [12]

$$\langle r_i(t) \rangle \propto \exp\left(-\sqrt{3}[B^3 - 3B^2s(t)]\varepsilon/D\right), \quad (14)$$

with the assumption of  $0 < B - s(t) \ll 1$ ,  $D = D_\xi + D_\eta$  and  $i = 1, 2, \dots, N$ . The ensemble-averaged correlation coefficient  $\langle \rho_{s,r} \rangle$  of a single neuron can be shown [12] that

$$\langle \rho_{s,r_i} \rangle \simeq \frac{\Delta\sigma_s}{[\exp(\Delta^2\sigma_s^2) - 1 + \sigma(D) \times \exp(V - \Delta^2\sigma_s^2)]^{1/2}}, \quad (15)$$

where  $\Delta = 3\sqrt{3}\varepsilon B^2/D$ ,  $V = 2\sqrt{3}\varepsilon B^3/D$  and  $\sigma(D)$  is a monotonically increasing empirical function of  $D$  [12].

According to (9), the variance of the network escape rate  $r(t) = \sum_{i=1}^N r_i(t)/N$  is given by

$$\overline{(r(t) - \overline{r(t)})^2} = \begin{cases} \overline{(r_i(t) - \overline{r_i(t)})^2}, & N = 1, \\ \frac{1}{N} \overline{[r_i^2(t) - r_i(t)]^2} + \frac{(N-1)}{N} \overline{r_i(t)r_j(t)}, & 1 < N < \infty, \\ \overline{r_i(t)r_j(t)}, & N = \infty. \end{cases}$$

Note that  $\overline{r_i(t)r_j(t)} = \overline{(r_i(t) - \overline{r_i(t)})^2}$  at the internal noise density  $D_\eta = 0$ , and the correlation gains of a single neuron and an infinite array all start from the same point, as shown in figures 3(d) and 5. Thus, we assume

$$\overline{r_i(t)r_j(t)} = \frac{D_\xi}{D} \times \overline{(r_i(t) - \overline{r_i(t)})^2}, \quad (16)$$

with a supposed coefficient  $D_\xi/D = D_\xi/(D_\xi + D_\eta)$  and without considering the interaction of the external noise  $\xi(t)$  and the array noise  $\eta_i(t)$  [30]. In this way, we have

$$\overline{(r(t) - \overline{r(t)})^2} = \overline{(r_i(t) - \overline{r_i(t)})^2} \times \left(\frac{D_\xi}{D} + \frac{D_\eta}{ND}\right). \quad (17)$$

By substituting (17) into equation (9) and considering (15), we have

$$\begin{aligned} \langle \rho_{s,r} \rangle &= \frac{\overline{s(t)r_i(t)}}{\sigma_s [\overline{(r_i(t) - \overline{r_i(t)})^2}]^{1/2}} \times \left(\frac{D}{D_\xi + (D_\eta/N)}\right)^{1/2} \\ &= \langle \rho_{s,r_i} \rangle \times \left(\frac{D}{D_\xi + (D_\eta/N)}\right)^{1/2} \\ &= \frac{\Delta\sigma_s}{[\exp(\Delta^2\sigma_s^2) - 1 + \sigma(D) \times \exp(V - \Delta^2\sigma_s^2)]^{1/2}} \times \left(\frac{D}{D_\xi + (D_\eta/N)}\right)^{1/2}, \end{aligned} \quad (18)$$

and the correlation gain  $G$  is

$$\langle G \rangle = \frac{\langle \rho_{s,r} \rangle}{\langle \rho_{s,s+\lambda} \rangle} = \frac{\Delta [(D/(D_\xi + (D_\eta/N))) \times (\sigma_s^2 + \sigma_\lambda^2)]^{1/2}}{[\exp(\Delta^2\sigma_s^2) - 1 + \sigma(D) \times \exp(V - \Delta^2\sigma_s^2)]^{1/2}}. \quad (19)$$

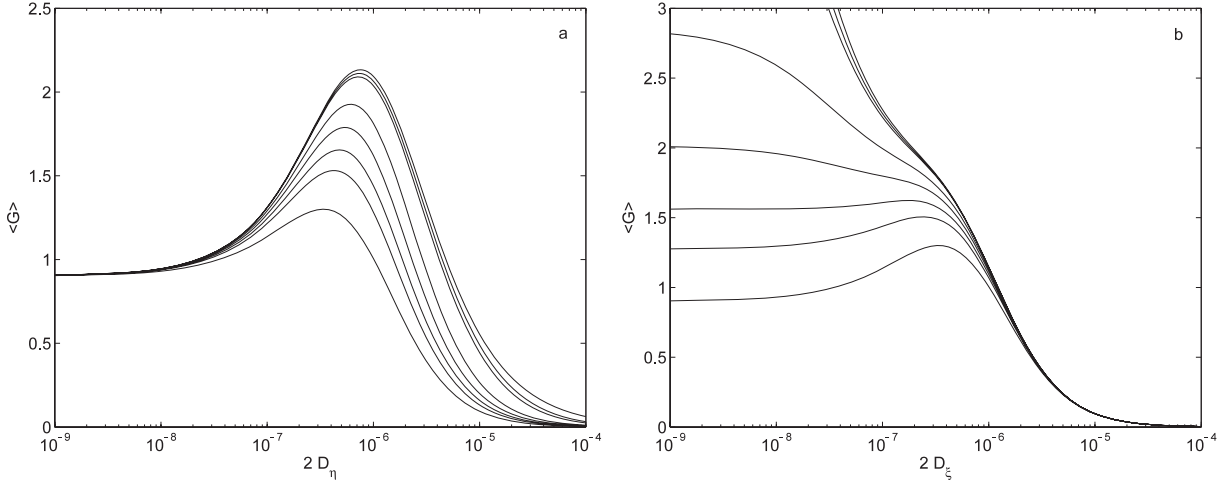


**Figure 6.** (a) Theoretical ensemble-average values of the correlation gain  $G = \rho_{s,r}/\rho_{s,s+\xi}$  as a function of the internal noise density  $D_\eta$  for the network with  $N = 1, 2, 3, 5, 10, 60, 120, \infty$  neurons (from the bottom up). Here, the fixed external noise density  $2D_\xi = 3 \times 10^{-7}$ . This configuration corresponds to figure 3(d); (b) theoretical ensemble-average values of the correlation gain  $G = \rho_{s,r}/\rho_{s,s+\eta}$  as a function of the external noise density  $D_\xi$  for the network with  $N = 1, 2, 3, 5, 10, 60, 120, \infty$  neurons (from the bottom up). Here, the given internal noise density  $2D_\eta = 3 \times 10^{-7}$ . This configuration corresponds to figure 4. When  $D_\eta$  is fixed ( $2D_\eta = 3 \times 10^{-7}$ ) and  $D_\xi$  varies, the term  $\lim_{N \rightarrow \infty} [D/(D_\xi + D_\eta/N)]^{1/2} = (D/D_\xi)^{1/2}$  in (19). Thus the correlation gain  $G$  tends to infinity at  $D_\xi = 0$ . The observable quantitative discrepancies between the analytical results of figure 4 and the numerical simulations of figures 3 and 4 indicate that this array SR theory needs to be improved in the future. In the theoretical prediction of (19),  $b = 0.07$ ,  $B = b_{\text{th}} - b = 0.0411$  and the empirical quadratic function  $\sigma(D) = c_1 D + c_2 D^2$  as well as [12, 15]. Here, we take constant coefficients  $c_1 = 4.2 \times 10^5$  and  $c_2 = 2.7 \times 10^3$  by nonlinear least-squares data fitting.

Figure 6 shows the theoretical ensemble-average values of the correlation gain  $G$  as a function of the internal or external noise for the neuronal array size  $N = 1, 2, 3, 5, 10, 60, 120$  and  $\infty$ . The appearance of array SR is clearly visible in figure 6. For a given noise density  $D_\eta$  or  $D_\xi$ , the correlation gain  $G$  increases as the array size  $N$  increases. More importantly, the regions of the correlation gain  $G > 1$  can be demonstrated by the above analytical descriptions of (9)–(19). The observable quantitative discrepancies between the analytical results of figure 6 and the numerical simulations of figures 3 and 4 are presented. A more accurate theory of array SR deserves to be developed in the future. However, this array SR theory captures well not only the nonmonotonic behavior of the correlation gain  $G$  as a function of the noise density for different neuronal array size  $N$ , but also the particular property of array SR, i.e. the correlation gain  $G > 1$ . Moreover, the array SR regions of internal noise density  $D_\eta$  or external noise density  $D_\xi$ , as shown in figure 6, agree well the numerical results of figures 3 and 4. When  $D_\xi$  is fixed and  $D_\eta$  varies, the correlation gain  $G$  starts at a common value at  $D_\eta = 0$ , as shown in figures 3(d) and 6(a).  $D_\eta$  starts from  $10^{-9}$  in the logarithmic scale in figure 6(a), but the correlation

gain  $G$  of (19) can be evaluated at  $D_\eta = 0$  with the same value. On the other hand, if we fix  $D_\eta$  and tune  $D_\xi$ , it is seen in figures 4 and 6(b) that the correlation gain  $G$  starts at different values at  $D_\xi = 0$ .  $D_\xi$  also starts from  $10^{-9}$  in the logarithmic scale in figure 6(b). The correlation gain  $G$  of (19) can be evaluated at  $D_\xi = 0$  for finite array size  $N$ , except  $N \rightarrow \infty$ , because the term  $\lim_{N \rightarrow \infty} [D/(D_\xi + D_\eta/N)]^{1/2} = (D/D_\xi)^{1/2}$  in (19). This array SR theory then confirms the noise-employed strategies by neuronal populations for a more efficient information representation. Additionally, the deduction of the escaping rate [12] requires the parameter  $B - s(t) > 0$ , thus this array SR theory does not describe the SR-type behavior induced by the suprathreshold stimulus ( $B = b_{\text{th}} - b < 0$  in figure 5). However, the numerical results shown in figure 5, as well as [20], confirms that the optimal coding strategy by tuning noise also plays a positive beneficial role for transmitting the suprathreshold stimulus through a summing FHN network.

## 6. Conclusions

In this paper, we studied the collective dynamics of an ensemble of FHN model neurons in the context of array SR. The performance of neuronal arrays with the finite and infinite size is investigated, numerically and theoretically. The internal noise in neuronal arrays plays a beneficial role in transmitting information, for given external environment noise. Moreover, this effect is also observed for suprathreshold stimuli. The collective dynamics of the neurons might be an optional strategy for a neuronal population. On the other hand, if the internal noise is fixed, the environmental noise can also invoke a similar array SR effect for more efficient information transfer, and this strategy might be adopted by a neuronal population to adapt to an ‘optimal’ noisy environment. Also, we can tune the environmental noise to make a neuronal population response more effective. Both numerical and theoretical results demonstrated the fact of the correlation gain exceeding unity, and the merit of these strategies for tuning noise deserves to be investigated more deeply. These results also suggest that certain levels of noise observed in biological sensory systems are an essential component of an optimal coding strategy, for example, in the condition of a population of sensory neurons operated to establish a neural representation of an analog stimulus from the environment.

## Acknowledgments

This work is sponsored by the NSFC (no. 60602040) and Taishan Scholar CPSP. Funding from the Australian Research Council (ARC) is gratefully acknowledged.

## References

- [1] Benzi R, Sutera A and Vulpiani A, *The mechanism of stochastic resonance*, 1981 *J. Phys. A: Math. Gen.* **14** L453
- [2] Benzi R, *Stochastic resonance in complex systems*, 2009 *J. Stat. Mech.* P01052
- [3] Gammaitoni L, Hänggi P, Jung P and Marchesoni F, *Stochastic resonance: a remarkable idea that changed our perception of noise*, 2009 *Eur. Phys. J. B* **69** 1
- [4] McDonnell M D, Amblard P O and Stocks N G, *Stochastic pooling networks*, 2009 *J. Stat. Mech.* P01012
- [5] McDonnell M D and Abbott D, *What is stochastic resonance? Definitions, misconceptions, debates, and its relevance to biology*, 2009 *PLoS Comput. Biol.* **5** e1000348
- [6] Chapeau-Blondeau F and Rousseau D, *Raising the noise to improve performance in optimal processing*, 2009 *J. Stat. Mech.* P01003

- [7] Patel A and Kosko B, *Optimal noise benefits in Neyman–Pearson and inequality-constrained statistical signal detection*, 2009 *IEEE Trans. Signal. Process.* **57** 1655
- [8] Gammaitoni L, Hänggi P, Jung P and Marchesoni F, *Stochastic resonance*, 1998 *Rev. Mod. Phys.* **70** 233
- [9] Cottone F, Vocca H and Gammaitoni L, *Nonlinear energy harvesting*, 2009 *Phys. Rev. Lett.* **102** 080601
- [10] Moss F, Pierson D and O’Gorman D, *Stochastic resonance: tutorial and update*, 1994 *Int. J. Bifurcation Chaos* **4** 1383
- [11] Longtin A, *Stochastic resonance in neuron models*, 1993 *J. Stat. Phys.* **70** 309
- [12] Collins J J, Chow C C and Imhoff T T, *Aperiodic stochastic resonance in excitable systems*, 1995 *Phys. Rev. E* **52** R3321
- [13] Lindner B, García-Ojalvo J, Neiman A and Schimansky-Geier L, *Effects of noise in excitable systems*, 2004 *Phys. Rep.* **392** 321
- [14] Moss F, Ward L M and Sannita W G, *Stochastic resonance and sensory information processing: a tutorial and review of application*, 2004 *Clin. Neurophysiol.* **115** 267
- [15] Collins J J, Chow C C and Imhoff T T, *Stochastic resonance without tuning*, 1995 *Nature* **376** 236
- [16] Henahan C, Collins J J, Chow C C, Imhoff T T, Lowen S B and Teich M C, *Information measures quantifying aperiodic stochastic resonance*, 1996 *Phys. Rev. E* **54** R2228
- [17] Chialvo D R, Longtin A and Muller-Gerking J, *Stochastic resonance in models of neuronal ensembles*, 1997 *Phys. Rev. E* **55** 1798
- [18] Tuckwell H C, Wan F Y M and Rodriguez R, *Analytical determination of firing times in stochastic nonlinear neural models*, 2002 *Neurocomputing* **48** 1003
- [19] Stocks N G, *Suprathreshold stochastic resonance in multilevel threshold systems*, 2000 *Phys. Rev. Lett.* **84** 2310
- [20] Stocks N G and Mannella R, *Generic noise-enhanced coding in neuronal arrays*, 2001 *Phys. Rev. E* **64** 030902
- [21] Hoch T, Wenning G and Obermayer K, *The effect of correlations in the background activity on the information transmission properties of neural populations*, 2005 *Neurocomputing* **65/66** 365
- [22] McDonnell M D, Stocks N G, Pearce C E M and Abbott D, 2008 *Stochastic Resonance: From Suprathreshold Stochastic Resonance to Stochastic Signal Quantization* (Cambridge: Cambridge University Press)
- [23] Collins J J, Priplata A A, Gravelle D D, Niemi J, Harry J and Lipsitz L A, *Noise-enhanced human sensorimotor function*, 2003 *IEEE Eng. Med. Biol. Mag.* **22** 76
- [24] Priplata A, Niemi J, Henry J, Lipsitz L and Collins J, *Vibrating insoles and balance control in elderly people*, 2003 *Lancet* **362** 1123
- [25] Gailey P C, Neiman A, Collins J J and Moss F, *Stochastic resonance in ensembles of nondynamical elements: the role of internal noise*, 1997 *Phys. Rev. Lett.* **79** 4701
- [26] Schmid G, Goychuk I and Hänggi P, *Stochastic resonance as a collective property of ion channel assemblies*, 2001 *Europhys. Lett.* **56** 22
- [27] Blanchard S, Rousseau D and Chapeau-Blondeau F, *Noise enhancement of signal transduction by parallel arrays of nonlinear neurons with threshold and saturation*, 2007 *Neurocomputing* **71** 333
- [28] Chapeau-Blondeau F and Rousseau D, *Enhancement by noise in parallel arrays of sensors with power-law characteristics*, 2004 *Phys. Rev. E* **70** 060101(R)
- [29] Duan F, Chapeau-Blondeau F and Abbott D, *Noise improvement of SNR gain in parallel array of bistable dynamic systems by array stochastic resonance*, 2006 *Electron. Lett.* **42** 1008
- [30] Duan F, Chapeau-Blondeau F and Abbott D, *Stochastic resonance in a parallel array of nonlinear dynamical elements*, 2008 *Phys. Lett. A* **372** 2159
- [31] Choi M H, Fox R F and Jung P, *Quantifying stochastic resonance in bistable systems: response versus residence-time distribution functions*, 1998 *Phys. Rev. E* **57** 6335
- [32] McDonnell M D, Abbott D and Pearce C E M, *A characterization of suprathreshold stochastic resonance in an array of comparators by correlation coefficient*, 2002 *Fluct. Noise Lett.* **2** L213
- [33] Ripoll Massanés S and Pérez Vicente C J, *Nonadiabatic resonances in a noisy Fitzhugh–Nagumo neuron model*, 1999 *Phys. Rev. E* **59** 4490
- [34] Volkov E I, Ullner E, Zaikin A A and Kurths J, *Oscillatory amplification of stochastic resonance in excitable systems*, 2003 *Phys. Rev. E* **68** 026214
- [35] Keener J and Sneyd J, 1999 *Mathematical Physiology* (Berlin: Springer)
- [36] Wang Y and Wu L, *Noise-improved signal correlation in an array of autoregressive models of order one*, 2007 *Fluct. Noise Lett.* **7** L449
- [37] Luca C J, LeFever R S, McCue M P and Xenakis A P, *Behaviour of human motor units in different muscles during linearly varying contractions*, 1982 *J. Physiol.* **329** 113